Experimental Results of a Waste Heat Recovery System with Ethanol Using Exhaust Gases of a Light-duty Engine

EXPERIMENTAL RESULTS OF A WASTE HEAT RECOVERY SYSTEM WITH ETHANOL USING THE EXHAUST GASES OF A LIGHT-DUTY ENGINE

Jelmer Rijpkema[1*], Fredrik Ekström[2], Karin Munch[1], and Sven B. Andersson[1]

[1] Chalmers University of Technology,
Department of Mechanics and Maritime Sciences
412 96, Göteborg, Sweden
jelmer.rijpkema@chalmers.se

[2] Volvo Car Corporation
Propulsion Power Systems Research & Strategy
Göteborg, Sweden
fredrik.ekstrom@volvocars.com

* Corresponding Author

ABSTRACT

Organic Rankine cycle (ORC) waste heat recovery (WHR) systems have the potential to improve the efficiency of modern light-duty engines, especially at high-way driving conditions. This paper presents and discusses the experimental results of an engine connected to a compact ORC-WHR system with ethanol, suitable for integration in a modern passenger car. The aim is to show the added value of this ORC-WHR system for passenger cars by presenting the experimental results with the focus on the expander power output. The experimental setup consists of a Volvo Cars VEP-4 gasoline engine, which has an evaporator integrated in the exhaust pipe. During operation, one of two different states can be selected: electrical feedback (EFB) or mechanical feedback (MFB), where the expander can be either coupled to a 48V generator (EFB) or directly to the engine (MFB). Control strategies were developed to allow for operation of the system without interference of the driver. The results show that the current setup and control strategies can be successfully employed with significant expander power outputs for both MFB and EFB. The expander power outputs, similar for both states, go up to 2.5 kW, recovering 6.5 % of the available exhaust energy and giving more than 5 % improvement in fuel consumption.

1. INTRODUCTION

Regulations on emissions push the developments for cleaner internal combustion engines, where electrification/hybridization and engine efficiency improvements are popular methods to reduce the CO_2 emissions. Improving engine efficiency can be achieved by using waste heat recovery (WHR) to recover energy that otherwise would be lost. A promising way to recover this energy is by using an organic Rankine cycle (ORC), technology already established in the field of power generation for stationary applications (Colonna et al., 2015). In the ORC, an organic fluid is evaporated at elevated pressure and expanded, thereby generating power. Although other methods, e.g. turbo-compounding or thermo-electric generators (Lion et al., 2017), as well as other thermodynamic cycles, e.g. transcritical or flash cycles (Rijpkema et al., 2018a), are currently being used or studied for WHR, the ORC remains a favorite due to its excellent performance. And, even though, other heat sources in the engine show potential for WHR (Rijpkema et al., 2018b), the exhaust gas shows the highest potential, owing to the high temperature and high energy content of the exhaust gas. An overview of different studies (experimental and numerical) by Zhou et al. (2016) shows that between 3 and 7 % of additional power (relative to the engine power) can be achieved by recovering the heat from the coolant, exhaust or the combination of both. Oomori and Ogino (1993) reported using the engine for the evaporative cooling of R123, giving a 3 % improvement in fuel economy. A simulation study by Punov et al. (2015) shows a reduction of fuel consumption between 2 and 8 % for a range of velocities between 80 and 160 km/h in a 2L gasoline engine using water as the working fluid and the exhaust gas as the heat source. Also using water and

the exhaust, an experimental study by BMW showed up to 5 % additional power for velocities between 70 and 150 km/h (Freymann et al., 2012). Boretti (2012) reported between 2 and 8 % of fuel efficiency improvement for simulations of a hybrid vehicle using the exhaust and the engine coolant as the heat source. Ekström (2019) reported WHR as an excellent addition to hybrid technology, with simulations showing a reduction in fuel consumption of up to 7% in high-way driving conditions (>25 kW).

The results shown here contain measurements from an experimental setup consisting of a 2 L gasoline engine with two evaporators integrated in the exhaust with ethanol as the working fluid. The power from the ORC-WHR system can be either directly added to the engine as mechanical power or converted to electrical power using a generator. The goal of this paper is to evaluate the feasibility of the ORC-WHR system, designed to be integrated in a passenger car. The experimental results will focus on the recovered power in both electrical and mechanical state for a range of relevant engine operating points.

2. EXPERIMENTAL SETUP

The experimental setup, shown in Fig. 1, consists of a Volvo Cars VEP-4 gasoline engine (4-cylinder, 2.0L, turbocharged), where the exhaust gas downstream the turbocharger heats the working fluid, i.e. ethanol. The exhaust gas leaves the exhaust through two double helix heat exchangers, bypassing the first heat exchanger (evaporator 1) until the three-way catalyst (TWC) reaches the required temperature. In the cycle, the buffer tank is partly filled with liquid, allowing for changes in volume of the working fluid as well as ensuring there is liquid at the pump inlet. The working fluid leaves the piston diaphragm pump at an increased pressure, entering the evaporators, where the heat is added to the cycle before entering the 3-cylinder axial piston expander. During warm-up, the expander is not running and all the fluid passes through the expander bypass valve, after which it condensed and subcooled in the condenser before entering the tank. When the system is warm, has sufficient pressure and superheating, the expander is started with the help of the 48V electric generator, followed by a closing of the expander bypass valve. The clutch allows for switching between two operating states. With the clutch disengaged, the expander operates in the electrical feedback (EFB) state, meaning it is only coupled to the generator and producing electrical power. When the clutch is engaged, the system switches to the mechanical feedback (MFB) state, where the expander is directly coupled to the engine, running at 1.5 times the engine speed. Three safety valves have been installed to protect the components at three different pressure levels. More details on the experimental setup and design decisions can be found in Ekström (2019).

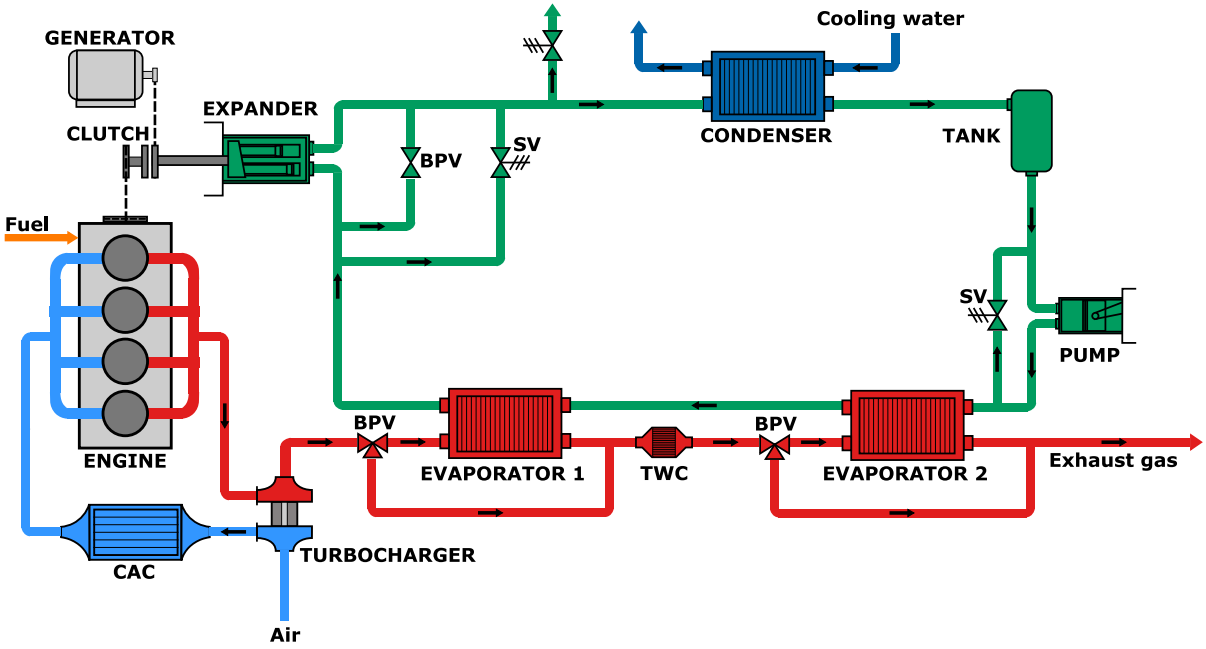

Figure 1: Schematic of the experimental setup for LD-WHR.

3. CONTROL STRATEGIES

The control of the system can be divided into four strategies, explained in more detail below, of which the corresponding diagrams are shown in Fig. 2. Not shown is the temperature control of the TWC.

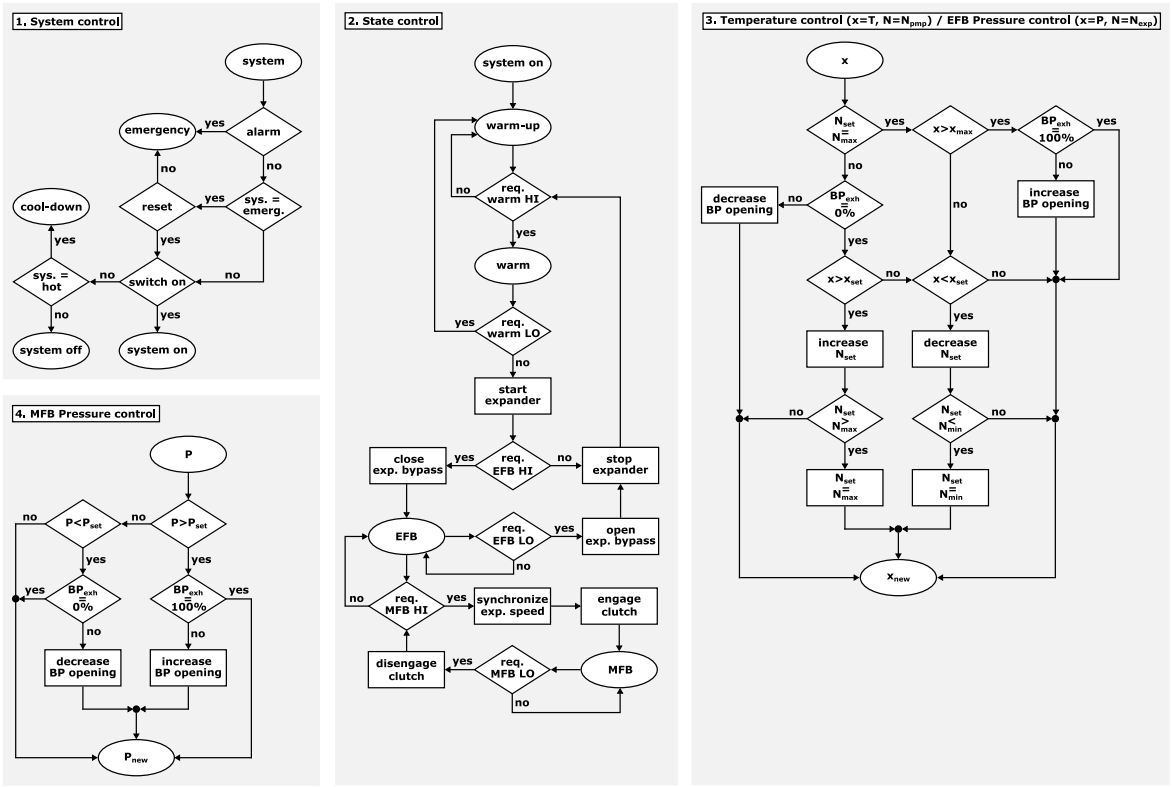

Figure 2: Control strategies.

1. **System control.** The system state is continuously checked and an alarm is triggered if the safety requirements are violated, e.g. if a maximum pressure/temperature limit is exceeded or a faulty sensor is detected. The system state is then set to emergency, which opens the expander bypass valve and stops the expander, while cooling down the system. The system can only return to the normal state if the reset button is activated. A digital switch is used to turn the system on and off. If the system is switched off while still hot, the system will switch to its cool-down state, meaning the pump is running at higher speeds to cool down the system.

2. **State control.** The system starts in the warm-up state and enters the warm state when the minimum requirements for this state (*warm_HI*) are met or exceeded. If during any state, the operating conditions drop below another set of minimum requirements (*warm_LO*), the system will return to warm-up. When the system is warm, the expander will start, assisted by the electric generator. When the requirements for EFB (*EFB_HI*) are satisfied, the expander bypass closes and the system is running in the EFB state, producing electrical power. If the MFB requirements are met, the expander speed synchronizes to the predicted MFB expander speed, the clutch closes, and the expander will transfer its power output directly to the engine. If the operating conditions fall below the MFB requirements (*MFB_LO*) it will switch back to the EFB state, from where it evaluates the warm requirements if conditions go below the minimum EFB requirements (*EFB_LO*).

3. **Temperature control / EFB Pressure control.** The evaporator outlet temperature in both EFB and MFB states is controlled using the pump speed. A higher pump speed means more mass flow, meaning a lower evaporator outlet temperature. The pump speed is controlled within a minimum and maximum speed, which cannot be exceeded. Also, if the temperature exceeds a specified maximum value, the exhaust bypass will open, reducing the heat transfer to the system, thus

preventing a higher temperature in the system. In an analogous manner, for the EFB state, the expander inlet pressure is controlled using the expander speed, where an increase in expander speed, means a reduction of the pressure.

4. **MFB Pressure control.** In the MFB state, the expander is coupled to the engine, making the expander speed is dependent on the engine speed which can, therefore, not be controlled. Therefore, the only way to regulate the pressure in the system, is to open and close the exhaust bypass valve, effectively increasing and decreasing the heat transfer to the system. The temperature control for the TWC works according to the same principle, albeit that the exhaust bypass is opened to increase the temperature and closed to decrease it. In the current setup the use of evaporator 1 led to excessive temperatures and, therefore, evaporator 1 was continuously bypassed.

4. RESULTS

The results are discussed in three separate sections, first showing the engine operating conditions, followed by the results for the MFB and EFB state. The cycle constraints employed in the control strategies are shown in in Table 1 as well as a number of cycle conditions.

Table 1: Cycle constraints and conditions.

Cycle constraints			
Expander speed	min	500	RPM
	max	3750	RPM
Pump speed	min	100	RPM
	max	1000	RPM
Expander inlet pressure	set	25	bar
	max	40	bar
Evaporator outlet temperature	set	230	°C
	max	300	°C

Cycle conditions		
Ambient temperature	21	°C
Ambient pressure	1.013	bar
Pump inlet temperature	35 – 45	°C
Condenser inlet pressure	1.3 – 1.9	bar
Condenser outlet pressure	1.2 – 1.4	bar
Condensation temperature*	83 – 95	°C

* Derived from condenser inlet and outlet pressures.

4.1 Engine

Fig. 3 shows the investigated range of engine speed and torque with the corresponding exhaust gas mass flows and temperatures, where the black dots represent the actual measurement points. The maximum engine speed was constrained by the maximum expander speed and the engine was limited to operate between 20 and 45 kW of power due to constraints on the mass flow range. The pump size did not allow for the smaller mass flow rates needed to sufficiently superheat the fluid at low engine operating points, while instable pump operation prevented pump speeds higher than the specified maximum.

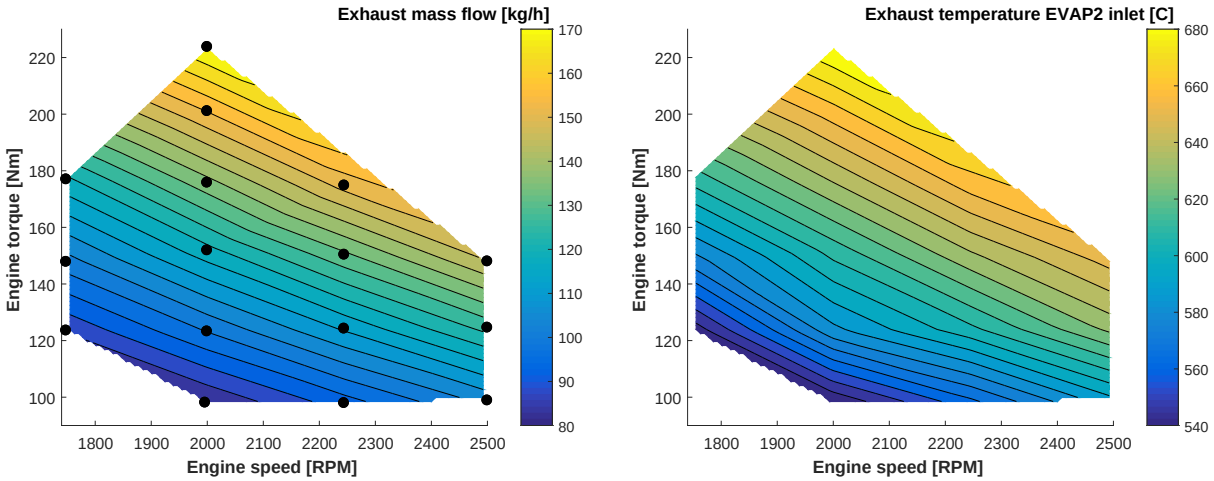

Figure 3: Exhaust mass flow and temperature at the inlet of evaporator 2. The black dots represent the actual measurement points.

4.2 Mechanical feedback (MFB)

The heat input in the cycle is dependent on the engine operating point, i.e. a higher engine power means more heat transfer to the working fluid. The temperature control tries to reach the specified set point by adjusting the pump speed, constrained by the minimum and maximum. In the left of Fig. 4 the expander inlet temperatures are shown, with the corresponding mass flows on the right. Since the expander is directly coupled to the engine, the expander speed cannot be controlled independently. This means that the pressure, shown in the left of Fig. 5, is a result of the given heat input, mass flow and expander speed. On the right of Fig. 5 the fuel savings are shown as ΔBSFC, defined in (1).

$$\Delta BSFC = BSFC - BSFC_{\text{mfb}} = 3.6 \cdot 10^9 \left(\frac{\dot{m}_\text{f}}{\dot{W}_\text{eng}} \right) - 3.6 \cdot 10^9 \left(\frac{\dot{m}_\text{f}}{\dot{W}_\text{eng}} \right)_\text{mfb} \tag{1}$$

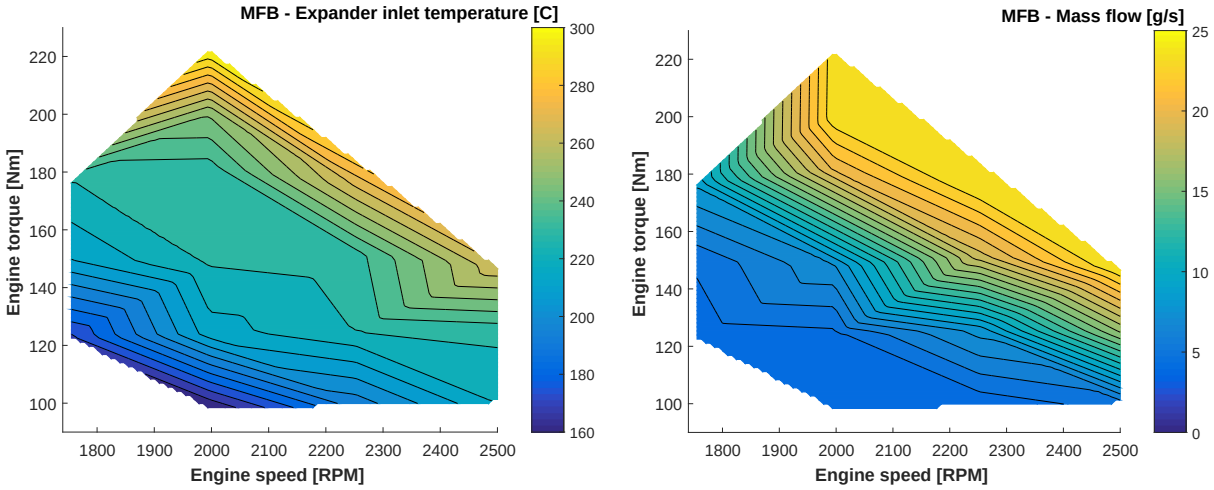

Figure 4: MFB - Expander inlet temperature and cycle mass flow.

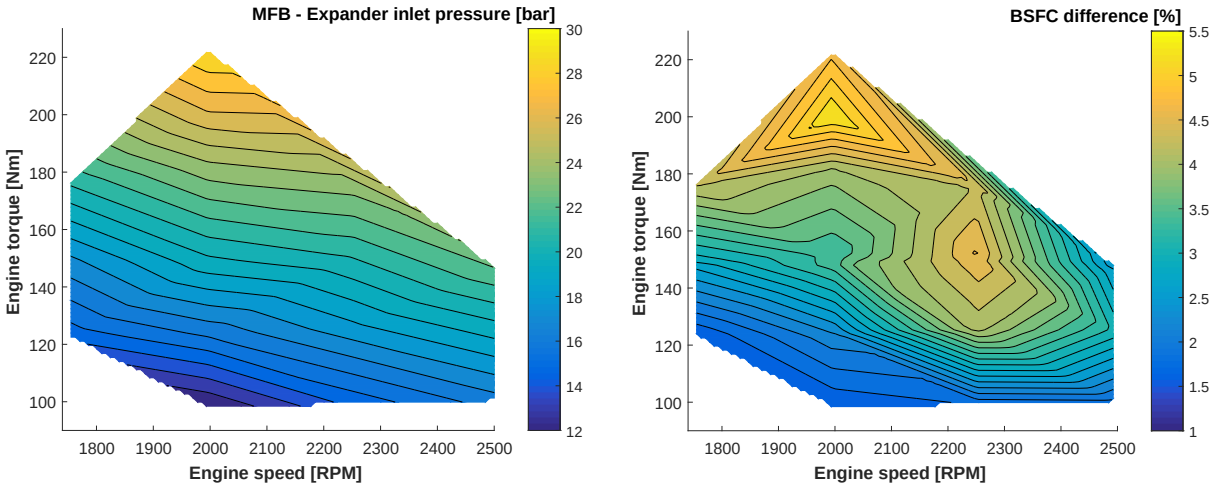

Figure 5: MFB - Expander inlet pressure and BSFC improvement.

Using the *BSFC* savings, the expander power can be calculated using Eq. (2) with the results shown on the left of Fig. 6. The right of Fig. 6 shows the total efficiency, which is the expander power divided by the total available energy in the exhaust flow (compared to ambient conditions), as defined in Eq. (3).

$$\dot{W}_{\text{exp,mfb}} = \dot{W}_\text{eng} \frac{\Delta BSFC}{BSFC} \tag{2}$$

$$\eta_{\text{tot,mfb}} = \frac{\dot{W}_{\text{exp,mfb}}}{\dot{Q}_{\text{tot}}} = \frac{\dot{W}_{\text{exp,mfb}}}{\dot{m}_{\text{exh}}(h_{\text{exh,ev1,in}} - h_{\text{exh,amb}})} \tag{3}$$

The MFB expander power includes all expander losses, where the mechanical losses can be included using the mechanical efficiency ($\eta_{\text{m,eng}}$) times the shaft expander power ($\dot{W}_{\text{sh,exp}}$), as shown in Eq. (4).

$$\dot{W}_{\text{exp,mfb}} = \eta_{\text{m,eng}} \dot{W}_{\text{sh,exp}} \tag{4}$$

The shaft expander power, shown in Eq. (5), is the expander efficiency (η_{exp}) times the extracted power from the fluid, which is the total extracted energy ($\Delta\dot{E}_{\text{exp}}$) minus the heat loss ($\dot{Q}_{\text{loss,exp}}$). The total extracted energy is simply the difference in total enthalpy flows between the expander in- and outlet.

$$\dot{W}_{\text{sh,exp}} = \eta_{\text{exp}} \left[\Delta\dot{E}_{\text{exp}} - \dot{Q}_{\text{loss,exp}}\right] = \eta_{\text{exp}} \left[\dot{m}_{\text{c}}(h_{\text{c,exp,in}} - h_{\text{c,exp,out}}) - \dot{Q}_{\text{loss,exp}}\right] \tag{5}$$

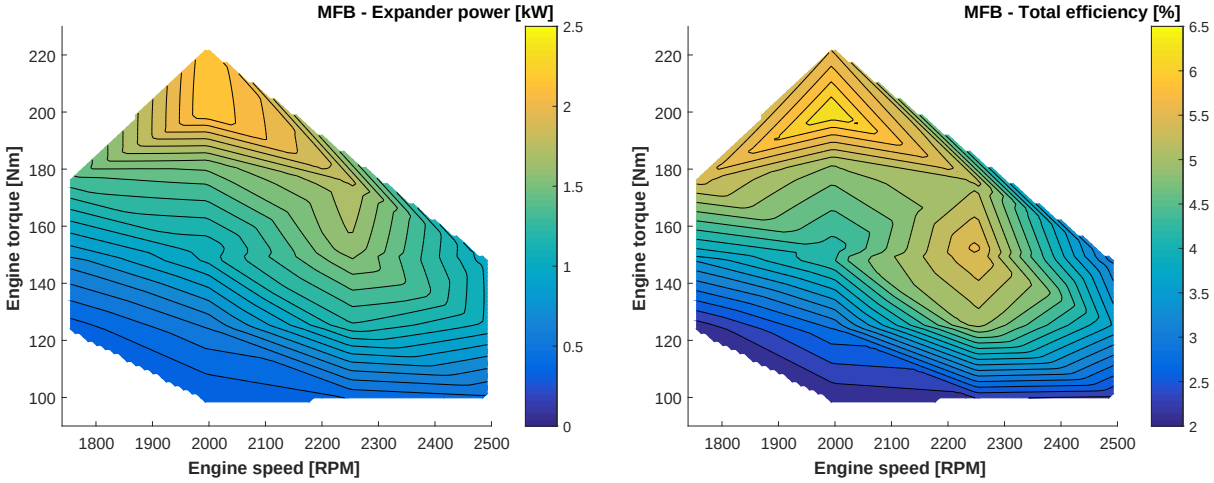

Figure 6: MFB - Expander power ($\dot{W}_{\text{exp,mfb}}$) and total efficiency ($\eta_{\text{tot,mfb}}$).

4.3 Electrical feedback (EFB)

The previously presented engine operating points were run for the EFB state using the cycle constraints given in Table 1. As with MFB, the pump speed was used to control the temperature, but now the expander speed could also be used to control the cycle pressure. The resulting expander power and total efficiency are shown in Fig. 7.

The expander power shown in Fig. 7 is derived from measurements at the generator shaft, as defined in Eq. (6). For a fair comparison with the MFB expander power, the electrical losses should be included, but these were not measured in these experiments. Eq. (7) gives the relation between the EFB expander power ($\dot{W}_{\text{exp,efb}}$), the shaft generator power ($\dot{W}_{\text{sh,gen}}$) and the shaft expander power ($\dot{W}_{\text{sh,exp}}$). The definition for the corresponding total efficiency is shown in Eq. (8).

$$\dot{W}_{\text{sh,gen}} = 2\pi \text{T}_{\text{gen}} \frac{N_{\text{gen}}}{60} \tag{6}$$

$$\dot{W}_{\text{exp,efb}} = \eta_{\text{el,gen}} \dot{W}_{\text{sh,gen}} = \eta_{\text{el,gen}} \eta_{\text{m,gen}} \dot{W}_{\text{sh,exp}} \tag{7}$$

$$\eta_{\text{tot,efb}} = \frac{\dot{W}_{\text{sh,gen}}}{\dot{Q}_{\text{tot}}} \tag{8}$$

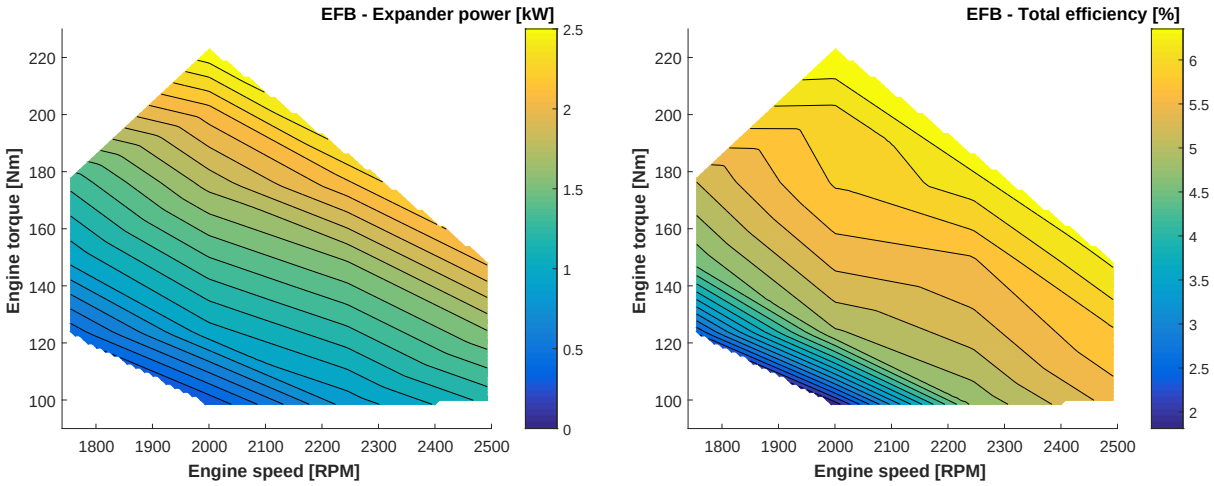

Figure 7: EFB - Expander power ($\dot{W}_{sh,gen}$) and total efficiency ($\eta_{tot,efb}$).

In the previous results, the expander speed was varied to obtain the specified pressure set point. A better strategy might be to vary the speed at different engine operating points to obtain the maximum expander power. For this purpose, the expander speed was varied for three engine operating points, shown in Table 2 with the corresponding exhaust mass flows and temperatures.

Table 2: EFB - Engine operating points.

#	N_{eng} [RPM]	T_{eng} [Nm]	$\dot{W}_{eng}$ [kW]	$\dot{m}_{exh}$ [kg/h]	$T_{exh,ev2,in}$ [C]
1.	1750	125	22.9	88	537
2.	2000	150	31.4	120	611
3.	2250	175	41.2	152	664

The resulting expander power outputs and corresponding expander inlet pressures are shown in Fig. 8, together with the speed for the MFB state at the corresponding engine operating point. The results show that only at the lowest engine power (23 kW), the expander power is near the optimum, while for the other engine powers going to higher expander speeds might increase the expander power output. As expected the pressure drops gradually with an increase in expander speed.

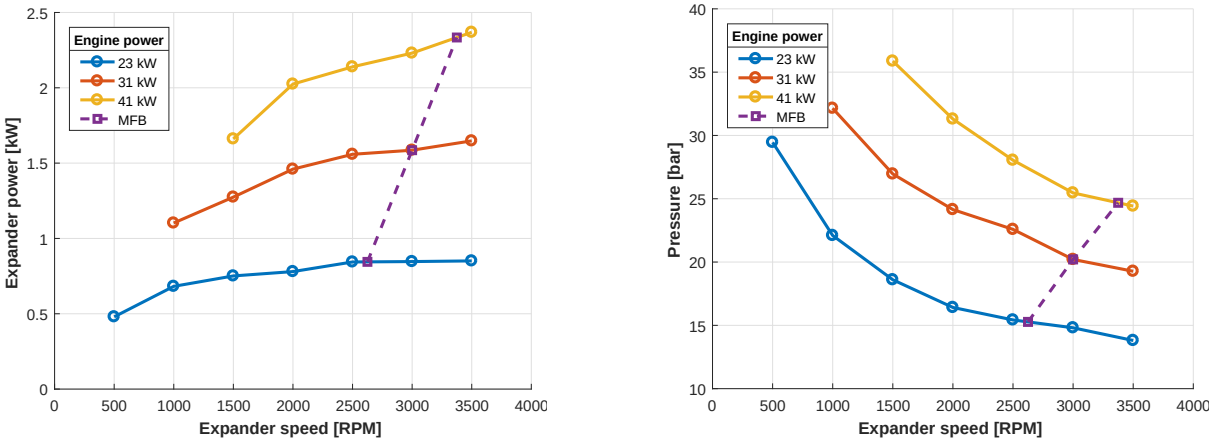

Figure 8: EFB - Expander power ($\dot{W}_{sh,gen}$) and expander inlet pressure.

The results show that the MFB and EFB expander power are similar, where in MFB the optimum power is more localized, since the expander speed cannot be controlled, in contrast to the EFB state. As presented, varying the expander speed can be used to further optimize the expander power output in EFB.

5. DISCUSSION

The experience, gained by running the experimental setup, leads to reflections that are valuable for future experiments. Below are the most important points of discussion.

- The range of investigated engine operating points was mainly limited by the available mass flow in the cycle. At the lower engine powers (<20 kW), the pump size was too big to ensure sufficient superheating. One way to overcome this limitation, is the use of a pump bypass valve, allowing part of the flow to recirculate back to the pump inlet. For the higher engine powers (>40 kW), instabilities in the flow prevented the pump to reach higher speeds. These instabilities are most likely caused by the low pressure at the pump inlet, which leads to either air infiltration or cavitation. To try to prevent this, the condensing pressure will be increased in future experiments.
- For this set of experiments, the temperature set point at the evaporator 2 outlet was kept constant (230 °C). However, improvements in expander power might be achieved by controlling the amount of superheating at the expander inlet instead.
- In the EFB state, the expander speed was used to control the pressure to the desired set point (25 bar). However, as shown by varying the expander speed for three engine operating points, the optimum expander power might correspond to a different pressure, depending on the engine operating point. This indicates that a strategy, other than using a fixed pressure set point, can be employed to obtain the maximum expander power. Also, in this study, the expander speed was limited to 3750 RPM. As suggested by Fig. 8, the optimum expander speed for the higher engine powers, might be situated at expander speeds larger than 3750 RPM.
- The expander power for MFB and EFB cannot be directly compared in this study. The MFB expander power is the net expander power ($\dot{W}_{\mathrm{exp,mfb}}$), which includes all losses, while the EFB expander power is the power measured at the electric generator ($\dot{W}_{\mathrm{sh.gen}}$), which does not include the electrical losses. For a fair comparison the net expander power in EFB ($\dot{W}_{\mathrm{exp,efb}}$) should be measured additionally and compared with the net expander power in MFB ($\dot{W}_{\mathrm{exp,mfb}}$).

6. CONCLUSIONS

The experimental setup of the ORC-WHR system was developed to be integrated into an existing passenger car platform. Control strategies were set up to function without interference of the driver for two different states: mechanical feedback (MFB) and electrical feedback (EFB). The possibility of switching between the two states (MFB and EFB) allows for a sophisticated control strategy to optimize the power of the WHR system during driving. The results in this study show that the current setup and control strategies can be successfully employed with significant expander power outputs for both MFB and EFB, leading to notable reductions in fuel consumption. With hybridization especially effective at city driving conditions (Ekström, 2019), the WHR system is a promising complementary technology at high-way driving conditions with possible fuel savings up to 5 %.

MFB and EFB give comparable expander power outputs up to 2.5 kW, recovering up to 6.5 % of the total available energy in the exhaust. The EFB shows a slightly higher power output, but the electrical losses are not measured. In MFB the expander speed cannot be controlled, therefore the corresponding pressure as well as expander output are determined by the heat input in the cycle. In the EFB state, the expander speed can be used to control the pressure in the system, where the speed giving the optimum expander power depends on the engine operating point.

ACKNOWLEDGMENTS

This research was made possible by funding provided by the Strategic Vehicle Research and Innovation Programme (FFI). The authors would also like to thank the academic and industrial partners in the WHR project, and in particular Volvo Cars, who provided the experimental setup. Also, special thanks go out to Ingo Friedrich and Robert Mollik from IAV GmbH for their calibration of the control system.

NOMENCLATURE

$BSFC$	brake specific fuel consumption	(g/kWh)
$\dot{E}$	energy transfer rate	(W)
h	specific enthalpy	(J/kg)
$\dot{m}$	mass flow	(kg/s)
N	rotational speed	(RPM)
$\dot{Q}$	heat transfer rate	(W)
$\dot{W}$	power	(W)

Greek symbols

η	efficiency	(-)
T	torque	(Nm)

Subscripts

amb	ambient
c	cycle
el	electrical
eng	engine
ev	evaporator
exh	exhaust
exp	expander
f	fuel
gen	generator
sh	shaft
tot	total
m	mechanical
pmp	pump

Abbreviations

bp	bypass
bpv	bypass valve
efb	electric feedback
evap	evaporator
ld	light-duty
mfb	mechanical feedback
orc	organic Rankine cycle
sv	safety valve
twc	three-way catalyst
whr	waste heat recovery

REFERENCES

Boretti, A. (2012). Recovery of exhaust and coolant heat with R245fa organic Rankine cycles in a hybrid passenger car with a naturally aspirated gasoline engine. *Applied Thermal Engineering*, 36(1).

Colonna, P., Casati, E., Trapp, C., Mathijssen, T., Larjola, J., Turunen-Saaresti, T., and Uusitalo, A. (2015). ORC Power Systems: From the Concept to Current Technology, Applications, and an Outlook to the Future. *Journal of Engineering for Gas Turbines and Power*, 137(10).

Ekström, F. (2019). A mild hybrid SIDI turbo passenger car engine with Rankine waste heat recovery. *SAE Technical Paper 2019-24-0194*.

Freymann, R., Ringler, J., Seifert, M., and Horst, T. (2012). The Second Generation Turbosteamer. *MTZ worldwide*, 73(2).

Lion, S., Michos, C. N., Vlaskos, I., Rouaud, C., and Taccani, R. (2017). A review of waste heat recovery and Organic Rankine Cycles (ORC) in on-off highway vehicle Heavy Duty Diesel Engine applications. *Renewable and Sustainable Energy Reviews*, 79.

Oomori, H. and Ogino, S. (1993). Waste heat recovery of passenger car using a combination of rankine bottoming cycle and evaporative engine cooling system. *SAE Technical Paper 930880*.

Punov, P., Evtimov, T., Milkov, N., Descombes, G., and Podevin, P. (2015). Impact of Rankine cycle WHR on passenger car engine fuel consumption under various operating conditions. In *The 28th international conference on Efficiency, Cost, Optimization, Simulation and Environmental Impact of Energy Systems - ECOS 2015*.

Rijpkema, J., Andersson, S., and Munch, K. (2018a). Thermodynamic Cycle and Working Fluid Selection for Waste Heat Recovery in a Heavy Duty Diesel Engine. *SAE Technical Paper 2018-01-1371*.

Rijpkema, J., Munch, K., and Andersson, S. B. (2018b). Thermodynamic potential of twelve working fluids in Rankine and flash cycles for waste heat recovery in heavy duty diesel engines. *Energy*, 160.

Zhou, F., Dede, E., and Joshi, S. (2016). Application of Rankine Cycle to Passenger Vehicle Waste Heat Recovery - A Review. *SAE International Journal of Materials and Manufacturing*, 9(2).